Formation of Multi-Channel Collagen Gels Investigated Using Particle Tracking Microrheology

Yonemoto, Junta
Graduate School of Science, Kyushu University

Maki, Yasuyuki
Faculty of Science, Kyushu University

Koh, Isabel
RIKEN (The Institute of Physical and Chemical Research)

Furusawa, Kazuya
Department of Environmental and Food Sciences, Fukui University of Technology

他

出版情報：Biomacromolecules. 22 (9), pp.3819-3826, 2021-08-03. American Chemical Society
バージョン：

Formation of Multi-Channel Collagen Gel Investigated Using Particle Tracking Microrheology

Junta Yonemoto[1], Yasuyuki Maki[2]*, Isabel Koh[3], Kazuya Furusawa[4], Masahiko Annaka[2]

[1] Graduate School of Science, Kyushu University, 744 Motooka, Nishi-ku, Fukuoka, Fukuoka, 819-0395, Japan

[2] Faculty of Science, Kyushu University, 744 Motooka, Nishi-ku, Fukuoka, Fukuoka, 819-0395, Japan

[3] RIKEN (The Institute of Physical and Chemical Research), 2-1 Hirosawa, Wako, Saitama, 351-0198, Japan

[4] Department of Environmental and Food Sciences, Fukui University of Technology, Gakuen 3-6-1 Fukui, Fukui, 910-8505, Japan

ABSTRACT: Collagen is one of the most common materials used to form scaffolds for tissue engineering applications. The multi-channel collagen gel (MCCG) obtained by the dialysis of an acidic collagen solution in a neutral buffer solution has a unique structure, with many capillaries of diameters several tens to a few hundred micrometers, and could be a potential candidate as a biomimetic scaffold for three-dimensional tissue engineering. In the present study, the formation of MCCG was investigated by *in situ* rheological measurements based on a particle tracking method (particle tracking microrheology, PTM). PTM enabled us to measure changes in the rheological properties of collagen solutions under the continuous exchange of substances during dialysis. When an observation plane was set perpendicular to the direction of gel growth, we first observed convectional flow of the collagen solution, followed by phase separation and gelation. We showed that the structure of the MCCG originated from the transient structure formed during the initial stage of viscoelastic phase separation and was fixed by the subsequent gelation.

1. INTRODUCTION

Collagen is the most abundant structural protein in animals and has a wide range of food, cosmetics, and medical applications.[1] Because collagen is the major protein found in extracellular matrices, collagen gels are a suitable material for constructing scaffolds for tissue engineering and three-dimensional (3D) cell culture.[2] Collagen gels are typically obtained by the incubation of collagen solutions under physiological pH or temperatures. Collagen molecules are soluble under acidic conditions below the isoelectric point. The neutralization of acidic collagen solutions by the addition of neutral buffer solutions at room temperature induces fibrillogenesis of collagen, resulting in gelation.[3-6] Recently, Furusawa et al. reported that the dialysis of an acidic collagen

solution in neutral phosphate buffer led to a gel that showed a unique structure, with many capillaries (or channels) of diameters several tens to a few hundred micrometers (referred to as multi-channel collagen gel, MCCG).[7] The multi-channel (MC) structure is reminiscent of the anisotropic hierarchical structures of biological tissues; therefore, MCCG could be a potential candidate for fabricating a biomimetic scaffold for 3D tissue engineering.[8-11]

In the formation of MCCG using the dialysis method, gelation began on the dialysis membrane where the collagen solution first came into contact with the buffer solution, and then proceeded as the neutralized region spread in one direction (directional neutralization) and a gelling front propagated accordingly (Fig. S1 of Supporting Information). The MC structure also appeared near the dialysis membrane first and then developed along the direction of the gel growth. In the resultant MCCG, the capillaries were aligned, in parallel, in the same direction.[7] The formation of MC structures similar to MCCG induced by the directional gelation process has been reported for other biopolymers.[12-17] The mechanism for the MCCG formation was proposed in the previous study; the development of the MC structure was attributed to spinodal decomposition, with the subsequent gelation preventing the structure from further coarsening.[7] Therefore, information about the dynamics of phase separation and gelation during the MCCG formation process are required for fine-tuning the number and size of the capillaries in MCCG, which would be essential for designing 3D tissue engineering scaffolds. The dynamics of the MC structure formation was investigated by microscopy in previous studies[7,10] but rheological approach necessary for clarifying the gelation dynamics has not been explored. However, rheological characterization of MCCG formation is difficult for the following reasons. The first reason is spatial inhomogeneity due to the phase separation; conventional rheological measurements only give rheological properties averaged over the material, not those of each phase. The second reason is that the gelation proceeds under the continuous exchange of substances during dialysis; the gelling system should be kept in contact with the dialysate, without interfering with the measurement. The third reason is that phase separation and gelation do not occur uniformly throughout the system; the rheological change should be measured locally in the region where the phase separation and the gelation occur. As shown later, these requirements can be satisfied by using a particle tracking microrheology (PTM) method.

For PTM measurement, the motion of microparticles dispersed in a sample is observed under a microscope, and the rheological properties of the sample are obtained by analyzing the trajectories of the particle centers.[18] The trajectories of the particles in the field of view reflect the rheology of their respective microenvironments and therefore contain information about the homogeneity/inhomogeneity of the system.[18,19] Thus, PTM is suitable for characterizing phase-separated systems such as MCCG. Another advantage of PTM is that we can measure rheological properties of a sample without retrieving it from the sample chamber, as it is a

contactless measurement technique. PTM allows us to carry out *in situ* rheological measurements of the MCCG formation process during dialysis. If an observation plane is set perpendicular to the direction of gel growth, changes in the rheological properties due to the phase separation and gelation can be measured when the phase separation and gelation fronts, respectively, pass through the observation plane. In the present study, the formation of MCCG was investigated by PTM and confocal laser scanning microscopy (CLSM). The initial conditions for the formation of the MC structure and the gelation were determined by CLSM and PTM, respectively. The PTM measurements of the MCCG formation process revealed that gelation occurred immediately after the formation of the MC structure, which was preceded by macroscopic flow of the collagen solution.

2. EXPERIMENTAL SECTION

2.1 Preparation of Collagen Gels

Solutions of atelocollagen at concentrations ranging from 1.0 to 5.0 mg/mL were prepared by diluting 5 mg/mL AteloCell IPC-50 collagen solution (Koken Co., Ltd, Japan) with 1 mM hydrochloric acid (Wako Pure Chemical Industries, Ltd., Japan). Phosphate buffer solutions at different pH values, from 6.0 to 8.0, and a constant ionic strength (73 mM) were prepared by dissolving disodium hydrogen phosphate and potassium dihydrogen phosphate (Wako Pure Chemical Industries, Ltd., Japan) in deionized water.

A sample chamber with a 5 × 5 × 1 mm well was fabricated by placing a 1-mm thick silicone rubber spacer with a 5-mm square hole on a 35-mm glass-bottomed dish (Fig. 1). After injecting the collagen solution into the well, a dialysis membrane was placed on the well and then a ring-shaped silicone rubber sheet and a glass tube were placed on the dialysis membrane. Gelation was initiated by pouring 2 mL of phosphate buffer into the glass tube. The gelation was observed from below with the aid of an inverted microscope.

2.2 CLSM Observation

Atelocollagen was immunofluorescently stained as follows and used for the CLSM observation of the collagen gels. AteloCell IPC-50 collagen solution, (Koken Co., Ltd, Japan), at 5 mg/mL, was mixed with 1 mg/mL anti-collagen type I (rabbit) antibody (Rockland Immunochemicals, Inc., PA, USA) at 1000:1 and incubated overnight at 4 °C. The solution was then mixed with 2 mg/mL goat anti-rabbit IgG labeled with Alexa Fluor 633 (Life Technologies Corp., OR, USA) at 1000:1 and incubated for 6 hours at 4 °C. Confocal fluorescence microscope images at 400 μm from the bottom of the sample chamber were obtained by CLSM (Carl Zeiss LSM880) equipped with a 10× objective lens. The observations were performed at 25 °C.

2.3 Preparation of Microparticles for PTM

Polyethylene glycol (PEG)-coated (PEGylated) microparticles were prepared as follows and used for the PTM measurement. PEG on the particle prevents adsorption of protein on the particle surface.[20-22] Carboxylated fluorescent polystyrene (PS) particles with a diameter of 0.49 μm (Polysciences, Inc., PA, USA) in 0.1 g of its aqueous suspension (2.5%) were washed with deionized water and redispersed in 0.9 mL deionized water. Stock solutions of 600 mM *N*-(3-dimethylaminopropyl)-*N*'-ethylcarbodiimide (EDC; Sigma-Aldrich) and 240 mM *N*-Hydroxysuccinimide (NHS; Sigma-Aldrich) in 50 mM 2-(*N*-morpholino) ethanesulfonic acid (MES; Dojindo Molecular Technologies, Inc., Japan) at pH 6 were prepared and 0.2 mL of each solution was added to the suspension. After 30 min under stirring, a solution of 0.3 g amino-terminated methoxy-PEG of 5.5 kDa (Rapp Polymere GmbH, Germany) in 1.4 mL MES (50 mM, pH 6) was added. After incubating overnight at 25 °C under stirring, the reaction was stopped by adding 100 μL of 100 mM glycine solution (Wako Pure Chemical Industries, Ltd., Japan). The suspension was centrifuged at 16000×g for 20 min and the supernatant was discarded. The PEGylated particles were washed via redispersion and centrifugation. Finally, the particles were redispersed in 3 mL deionized water and stored at 4 °C until use. Before and after modification, the particles were characterized by their hydrodynamic diameter and zeta potential, which were measured with the aid of a Malvern Panalytical Zetasizer Nano ZS instrument. The hydrodynamic diameter slightly increased (from 478 ± 4 to 536 ± 10 nm), and the zeta potential changed from -41.7 to -10.7 mV, indicating the covalent grafting of non-ionic PEG to the surface of the carboxylated PS particles.[22] The surface density of PEG on a PS particle was estimated to be 3.3 × 10^{13} cm^{-2} by nuclear magnetic resonance (NMR) measurement, as described in the Supporting Information.

2.4 PTM Measurement

During the PTM measurement, collagen solutions containing 2 × 10^{-4}% PEGylated fluorescent PS particles were used for the gel preparation. The motion of the fluorescent particles at 150–200 μm from the bottom of the sample chamber was observed using a fluorescence microscope (Nikon ECLIPSE TS-100F) equipped with a 60× objective lens and recorded by a CMOS camera at a frame rate of 24 fps and exposure time of 8.3 ms. The displacement of the particle centers was measured by analyzing the video images using ImageJ/FIJI software with a particle track and analysis plugin (https://github.com/arayoshipta/projectPTAj). The rheology of the sample during the gelation process can be represented by the mean square displacement (MSD) of each particle:

$$\langle \Delta x_i^2(\tau) \rangle = \langle |x_i(t+\tau) - x_i(t)|^2 \rangle_t \qquad (1)$$

and the ensemble-averaged MSD:

$$\langle \Delta x^2(\tau) \rangle = \frac{1}{N} \sum_{i=1}^{N} \langle \Delta x_i^2(\tau) \rangle, \qquad (2)$$

where $x_i(t)$, τ and N are the centroid coordinate of the ith particle at time t, the lag time, and the number of particles, respectively, while $\langle \quad \rangle_t$ represents the average over time t.[18] The spatial resolution ε, which gives the static error,[18] was determined to be 10.3 nm by measuring the MSD of particles immobilized in a strong gel of 25 wt% Pluronic F-127 (BASF SE, Germany) in water. The measurements were performed at 25 °C.

In general, the MSD of a particle in Brownian motion in a viscous fluid is proportional to τ, as follows:

$$\langle \Delta x^2(\tau) \rangle = 2D\tau, \qquad (3)$$

where D is a diffusion coefficient.[18] On the other hand, the MSD of a particle in an elastic solid is independent of τ, as follows:

$$\langle \Delta x^2(\tau) \rangle = \frac{k_B T}{\kappa} \qquad (4)$$

because it is effectively held in place by a spring with a spring constant κ.[18] Therefore, defining the slope α of the double logarithmic plot of the MSD as

$$\alpha = \frac{d \log \langle \Delta x^2(\tau) \rangle}{d \log \tau}, \qquad (5)$$

the gelation can be represented by the change in α, from 1 to 0.

3. RESULTS AND DISCUSSION

3.1 Conditions for MC Structure Formation and Gelation

To determine the conditions for the formation of the MC structure, CLSM observations were performed 30 min after the start of the dialysis for the sample of different collagen concentrations, dialyzed against buffers at different pH values. The results are shown in Fig. S3 of Supporting Information. The MC structure was observed with higher collagen concentrations and higher buffer pH values. For example, Figure 2 shows a CLSM image of the sample formed using 5.0 mg/mL collagen, prepared with a buffer of pH 7.4. The bright and dark areas indicate high and low collagen concentrations, respectively. A concentrated phase (collagen-rich phase) formed a continuous phase, with domains of a dilute phase (solvent-rich phase) corresponding to the capillary structure dispersed in the concentrated phase. On the other hand, a homogeneous structure was observed with lower collagen concentrations or lower buffer pH values as shown in Fig. S3 of Supporting Information.

To determine the conditions for the gelation of the collagen solutions, PTM measurements were carried out 30 min after the start of the dialysis for different collagen concentrations and different

buffer pH values. The results are shown in Fig. 3 and Fig. S4 of Supporting Information. Fig. 3 shows the ensemble-averaged MSD of 3.0 mg/mL collagen solution dialyzed against buffers at different pH values. As described later, particle dynamics in the present system could be heterogeneous in some cases and each MSD curve in Fig. 3 represents a behavior of the majority of the particles. At pH 6.0, the value of the slope α of the double logarithmic plot was close to 1, indicating the collagen solution behaved as a viscous fluid. At pH values higher than 6.5, the values of α were almost zero, which resulted from the formation of elastic gels. Thus, the gelation occurred at a pH value between 6.0 and 6.5. The MSD curves for 1.0 and 5.0 mg/mL collagen solutions at different pH values are shown in Fig. S4, which indicates that gelation occurred at a pH value between 6.5 and 6.8 for 1.0 mg/mL collagen, and between 6.0 and 6.5 for 5.0 mg/mL collagen, respectively.

Combining the results of the CLSM and PTM experiments, a "phase diagram" representing conditions for the MC structure formation and gelation was constructed (Fig. 4). The boundary of the phase separation, i.e. the formation of the MC structure, did not coincide the sol-gel boundary. Thus, the final state of the collagen sample after the dialysis process depended on the collagen concentrations and the pH values of the dialysate solution and was classified into three types: homogeneous solution, homogeneous gel, and MCCG.

3.2 Dynamics of MCCG Formation

The MCCG formation process was investigated under the conditions of 5.0 mg/mL collagen and a buffer pH of 7.4. Figure 5 shows the variation in MSD with time t_d after the start of the dialysis of the collagen solution. The MSD curves in Fig. 5 were ensemble-averaged for the particles showing a typical behavior. Initially, a fluid-like behavior ($\alpha \cong 1$) was observed (t_d = 2 min and 4 min). Then, the shape of the MSD curve varied as $\alpha \cong 1$ for shorter τ and $\alpha \cong 2$ for longer τ (t_d = 6 min and 8 min). In general, a relationship $0 \leq \alpha \leq 1$ holds for the MSD of particles in Brownian motion. However, the value of α can be greater than 1 when there exists a drift of particles caused by a macroscopic flow or convection. For particles in a fluid under flow with a constant velocity V, for example, the MSD curve shows a crossover from $\alpha = 1$ to $\alpha = 2$ as[23]

$$\langle \Delta x^2(\tau) \rangle = 2D\tau + V^2\tau^2. \qquad (6)$$

According to eq. (6), the crossover behavior observed at t_d = 6 min and 8 min indicates that the collagen solution behaved as a viscous fluid and macroscopic flow occurred. Finally, the gel was formed and an MSD suggestive of an elastic behavior ($\alpha \cong 0$) was observed ($t_\mathrm{d} \geq$ 10 min). A gradual change in α from 1 to 0 in the transition from a fluid to a gel was not observed, owing to the rather fast gel formation in the present study.

Differences in rheological characteristics before and after MCCG formation were clarified by a close inspection of the MSD of each particle. The MSD of each particle before gelation (t_d = 2

min) is shown in Fig. 6a. The MSD curves of each particle (gray lines) overlapped with each other, indicating that the microenvironments for the particles were equivalent, i.e., the system was homogeneous. The rheological properties were unchanged from those of the original collagen solution, because the MSD values were almost the same as those of the collagen solution (solid black line). After gelation (t_d = 40 min), the behaviors of the MSD of each particle could be classified into three groups (Fig. 6b), which is due to the inhomogeneity of the system. Most of the MSD curves (blue lines) exhibited an elastic behavior ($\alpha \cong 0$), corresponding to that of the particles trapped in the gel. In addition, there were some MSD curves (red lines) that showed a fluid-like behavior ($\alpha \cong 1$) and a few MSD curves (green lines) indicative of an intermediate behavior. The values of the MSD for the fluid-like behavior coincided with those of the MSD for water (dashed black line). Figure 7 shows a CLSM image of MCCG prepared with a collagen solution containing fluorescent particles. The majority of the fluorescent particles were found in a collagen-rich concentrated phase, but several were observed in the capillaries as a dilute phase. The MSDs of the elastic behavior and the fluid-like behavior (blue and red lines in Fig. 6b, respectively) were attributed to the particles in a concentrated phase in the gel state and those diffusing in the capillaries mainly filled with water, respectively. The MSD of the intermediate behavior (green lines) slightly increased with τ and leveled off at longer τ. This behavior is similar to that of the MSD seen for particles diffusing in a confined space.[24-26] The observed intermediate behavior could be ascribed to particles confined in a region with a sparse network surrounded by a dense network in the concentrated phase. As described in the Supporting Information, the approximate size of the region confining a particle was calculated to be 1.2–1.9 μm, from the plateau value of MSD (0.006–0.11 μm^2) at longer τ.

Figure 8a shows the variation of α during MCCG formation obtained from the ensemble-averaged MSD in the short τ region (0.03 s $\leq \tau \leq$ 0.2 s). In cases where different types of behaviors appeared, as shown in Fig. 6b, the MSD curves of the majority and those of the diffusing particles were analyzed separately; the results are represented by filled circles and open circles, respectively. Some of the MSD curves of the intermediate behavior have not been taken into account here. For $t_d \leq$ 8 min, the system was homogeneous and the values of α were approximately 1. In the time period of 8 min $< t_d <$ 10 min, bifurcation of the particle dynamics appeared. The α of a majority of the particles decreased, as can be seen from the filled circles, indicating the formation of a gel. On the other hand, the α of some particles remained unchanged even at $t_d \geq$ 10 min, as can be seen from the open circles; this is due to the particles in the capillaries. This is substantiated by the MSD values at τ = 0.09 s shown in Fig. 8b: the MSD values of the particles with $\alpha \cong 1$ at $t_d \geq$ 10 min (open circles) were close to the value of the particles in water (dashed line). The appearance of the bifurcation of the particle dynamics should coincide with the formation of the MC structure due to phase separation. Thus, the phase separation

and the gelation occurred during the same period of time, i.e., 8 min < t_d < 10 min. This result implies the pinning of the MC structure by gelation immediately following the formation of the MC structure by the phase separation.

Figure 9 shows the variation in α during MCCG formation from the ensemble-averaged MSD in the long τ region (0.5 s ≤ τ ≤ 2 s). The value of α was approximately 1 in the beginning and increased with time until it reached close to 2 at t_d = 8 min. This increase in α indicates that a macroscopic flow became more significant, as shown in Fig. 5. The value of α decreased rapidly during the time period of 8 min < t_d < 10 min, reflecting the cessation of the macroscopic flow. Following phase separation and gelation, α behaved in a similar way to that in the short τ region, as shown in Fig. 8a.

3.3 Mechanism for Macroscopic Flow

The MSD curves during the MCCG formation process revealed that a macroscopic flow of the collagen solution on the observation plane appeared soon after the start of dialysis, and gradually became more significant until just before the phase separation and the gelation (Fig.9). This indicates that the effect of the macroscopic flow became evident earlier than the formation of the MC structure. Figure 10 shows CLSM images during the formation of the MC structure. The formation of the MC structure started at t_d = 320 s and ended at t_d = 350 s. The phase separation time in CLSM (t_d = 5–6 min) apparently earlier than that in MPT (t_d = 8–10 min) is reasonable because the observation point of CLSM and PTM was different (400 μm and 150–200 μm from the bottom for CLSM and PTM, respectively), i.e., the phase separation front passed through the observation plane of CLSM earlier than that of PTM. Figure 10 indicates that the MC structure formation on the observation plane finished within 1 min. This result was consistent with the result of PTM that the bifurcation of the particle dynamics occurred within the measurement time interval of 2 min (Fig. 8a). Thus, the MC structure formation occurred relatively fast at the phase separation time of the observation point. In contrast, the macroscopic flow shown in Fig. 9 emerged soon after the start of the dialysis and persisted until the phase separation and gelation occurred.

The mechanism for the macroscopic flow observed earlier than the onset of the phase separation can be explained in the following way. As the phase separation front moved in accordance with the directional neutralization, a capillary structure elongated along the direction of the motion of the front (a movie in the Supporting Information). Near the capillary-growth point, fluid exchange between the collagen solution and the dialysate solution will occur, which may provoke convection of the collagen solution. Moreover, as shown in Fig. 11, in the area where the capillary structure was newly formed (shaded area), interdiffusion of collagen and solvent (red and blue arrows, respectively) should occur. This transport of substances may also induce convection of the collagen solution in the vicinity (red area) of the capillary-growth point. Such convection accounts for the

values of α in the long τ region that were more than 1, observed during the initial stage of the MCCG formation process (Fig. 5, Fig. 9).

3.4 Mechanism for MCCG Formation

In a preceding study, Furusawa et al. showed that capillary radius increased proportionally with $t_{\mathrm{d}}^{1/3}$ during the MCCG formation process and concluded that the formation of the MC structure was due to phase separation by spinodal decomposition.[7,10] Tsukada and Kurita carried out a two-dimensional numerical simulation of phase separation induced by a directional quench to the unstable region. They showed that a columnar pattern was formed parallel to the direction of spread of the quenched region, depending on the speed of the quenching front,[27] which supports the theory that MC structure formation is dominated by spinodal decomposition.

The neutralization of the acidic collagen solution increases the effective attractive interaction between collagen molecules. Thus, assuming that the buffer pH corresponds to the interaction parameter χ,[28] the boundary between the areas of MCCG and homogeneous gel, shown as a solid line in the "phase diagram" of Fig. 4, may represent a "spinodal line". In phase diagrams of binary systems in the plane of χ and composition ϕ, a critical point is located at the minimum of the spinodal line.[28] Because the solid line in Fig. 4 tends to decrease monotonically, the concentration range used in the present study would fall below the critical concentration. According to the Flory–Huggins theory of polymer solutions, the critical composition is given as $\phi_{\mathrm{c}} = \frac{1}{1+\sqrt{n}}$, where n is the degree of polymerization.[28] As the length, diameter, and degree of polymerization n of a triple-helical collagen molecule are approximately 300 nm, 1.5 nm, and 3000, respectively,[29,30] the value of ϕ_{c} is estimated to be 0.018 (equivalent to 17 mg/mL), which is larger than the concentration range used in the present study.

When polymer solutions at concentrations below the critical concentration undergo spinodal decomposition, droplets of a concentrated (polymer-rich) phase, which is the minority phase, should be formed in a dilute (solvent-rich) phase, which is the majority phase.[31] In contrast, during MCCG formation, droplets of a solvent-rich phase comprising the capillaries were dispersed in a gelled, collagen-rich phase comprising a continuous phase. This suggests that the formation of the MC structure is associated with viscoelastic phase separation,[32,33] as described below.

Viscoelastic phase separation is a type of phase separation in which the dynamics are significantly affected by viscoelastic effects; it is observed when dynamically asymmetric mixtures comprising slow and fast components, such as polymer solutions, are quenched deep into an unstable region of the phase diagram.[32,33] The pattern formation during viscoelastic phase separation is quite different from that seen in normal phase separation of fluid mixtures. During the initial stage, the usual increase in concentration fluctuation occurs. However, the viscoelastic effects

prevent the rapid growth of composition fluctuations that are characteristic of spinodal decomposition from proceeding further. This is because the slow component (polymers) cannot catch up with the deformation rate of the phase separation itself and starts to behave like a viscoelastic body. The less viscoelastic solvent-rich phase appears as droplets after a period of incubation, and then the number and size of droplets increases with time. The viscoelastic polymer-rich phase shrinks while expelling the solvent into the solvent-rich droplets, and thus its volume decreases with time. It forms a well-developed network structure during the volume shrinking process. The thin parts of the network structure become elongated and eventually break up. During the final stage, the system becomes more fluid-like, reflecting the slowing down of the phase separation due to the fact that the composition of both phases approaches their final equilibria. After a long time, the network structure of the polymer-rich phase eventually transforms into a droplet structure. This "phase inversion" behavior has been confirmed by experiments[34] and simulations.[35] The formation of the MC structure of MCCG can be explained as the formation of droplets of the solvent-rich phase in the polymer-rich phase during the initial stage of viscoelastic phase separation followed by pinning of the transient structure. The "phase diagram" in Fig. 4 shows that the gel line (dashed line) is outside of the boundary line of the formation of the MC structure and therefore the conditions for the MC structure formation automatically satisfied the conditions for gelation in the present study. Thus, the later stages of viscoelastic phase separation, such as formation of the well-developed network structure, phase inversion, and formation of polymer-rich droplets, were not observed because of the gelation that occurred immediately following the formation of the MC structure.

CONCLUSION

PTM was used to investigate MCCG formation induced by the dialysis of acidic collagen solutions in neutral buffer solutions. Conditions for the MC structure formation and gelation were determined by CLSM observation and PTM measurements, respectively. PTM enabled us to perform rheological measurements without retrieving the sample from the chamber, meaning that the CLSM and PTM experiments on the samples could be carried in the same dialysis chamber. Rheological changes in the MCCG formation process were measured using PTM without interrupting dialysis. The MSD curves for shorter τ provided information about the structure formation due to phase separation and gelation, whereas those for longer τ provided information about the appearance of the convectional flow of the collagen solution prior to phase separation and gelation. This demonstrates that PTM remains effective even if a certain level of particle drift is unavoidable. During the MCCG formation process, convection of the collagen solution appeared and gradually became significant. After incubation for some time, the convection suddenly stopped and then phase separation occurred, which was quickly followed by gelation. The phase diagram

showing the conditions necessary for the MC structure formation and gelation indicated that the formation of the MC structure could be attributed to droplet formation in a solvent-rich phase during the initial stage of viscoelastic phase separation, which was subsequently fixed by the gelation.

Supporting Information

Gelation of collagen induced by directional neutralization; estimation of the surface density of PEG on a PS particle using NMR measurement; conditions for the formation of the MC structure; conditions for the gelation; estimation of the size of the region confining a particle; and elongation of the capillary structure

ACKNOWLEDGMENTS

This work was supported by JSPS KAKENHI (Grants-in-Aid for Scientific Research) Grant Number 15K20906 and 18K05519.

REFERENCES

(1) Sionkowska, A.; Skrzyński, S.; Śmiechowski, K.; Kołodziejczak, A. The review of versatile application of collagen. *Polym. Adv. Technol.* **2017**, 28, 4-9.

(2) Van Vlierberghe, S; Dubruel, P.; Schacht, E. Biopolymer-based hydrogels as scaffolds for tissue engineering applications: a review. *Biomacromolecules* **2011**, 12, 1387-1408.

(3) Tran-Ba, K. H.; Lee, D. J.; Zhu, J.; Paeng, K.; Kaufman, L. J. Confocal rheology probes the structure and mechanics of collagen through the sol-gel transition. *Biophys. J.* **2017**, 113, 1882-1892.

(4) Shayegan, M.; Forde, N. R. Microrheological characterization of collagen systems: from molecular solutions to fibrillary gels. *Plos One* **2013**, 8, e70590.

(5) Gobeaux, F.; Mosser, G.; Anglo, A.; Panine, P.; Davidson, P.; Giraud-Guille, M.-M.; Belamie, E. Fibrillogenesis in dense collagen solutions: a physicochemical study. *J. Mol. Biol.* **2008**, 376, 1509-1522.

(6) Forgacs, G.; Newman, S. A.; Hinner, B.; Maier, C. W.; Sackmann, E. Assembly of collagen matrices as a phase transition revealed by structural and rheologic studies. *Biophys. J.* **2003**, 84, 1272-1280.

(7) Furusawa, K.; Sato, S.; Masumoto, J.; Hanazaki, Y.; Maki, Y.; Dobashi, T.; Yamamoto, T.; Fukui, A.; Sasaki, N. Studies on the formation mechanism and the structure of the anisotropic collagen gel prepared by dialysis-induced anisotropic gelation. *Biomacromolecules* **2012**, 13, 29-39.

(8) Koh, I.; Furusawa, K.; Haga, H. Anisotropic multi-channel collagen gel (MCCG) guides the

growth direction of the neurite-like processes of PC12 cells. *Sci. Rep.* **2018**, 8, 13901.

(9) Yahata, S.; Furusawa, K.; Nagao, K.; Nakajima, M.; Fukuda, T. Effects of three-dimensional culture of mouse calvaria-derived osteoblastic cells in a collagen gel with multichannel structure on the morphogenesis behaviors of engineered bone tissues. *ACS Biomater. Sci. Eng.* **2017**, 3, 3414-3424.

(10) Furusawa, K.; Mizutani, T.; Machino, H.; Yahata, S.; Fukui, A.; Sasaki, N. Application of multichannel collagen gels in construction of epithelial lumen-like engineered tissues. *ACS Biomater. Sci. Eng.* **2015**, 1, 539-548.

(11) Hanazaki, Y.; Masumoto, J.; Sato, S.; Furusawa, K.; Fukui, A.; Sasaki, N. Multiscale analysis of changes in an anisotropic collagen gel structure by culturing osteoblasts. *ACS Appl. Mater. Interfaces* **2013**, 5, 5937-5946.

(12) Maki, Y.; Furusawa, K.; Yamamoto, T.; Dobashi, T. Structure formation in biopolymer gels induced by diffusion of gelling factors. *J. Biorheol.* **2018**, 32, 27-38.

(13) Schuster, E.; Eckardt, J.; Hermansson, A-M.; Larsson, A.; Lorén, N.; Altskär, A.; Ström, A. Microstructural, mechanical and mass transport properties of isotropic and capillary alginate gels. *Soft Matter* **2014**, 10, 357-366.

(14) Despang, F.; Dittrich, R.; Gelinsky, M. Novel biomaterials with parallel aligned pore channels by directed ionotropic gelation of alginate: mimicking the anisotropic structure of bone tissue. In *Advances in Biomimetics*; George, A. Eds.; INTECH Open Access Publisher: London, 2011; p 349-372.

(15) Thumbs, J.; Kohler, H-H. Capillaries in alginate gel as an example of dissipative structure formation. *Chem. Phys.* **1996**, 208, 9-24.

(16) Sereni, N.; Enache, A.; Sudre, G.; Montembault, A.; Rochas, C.; Durand, P.; Perrard, M-H.; Puaux, J-P.; Delair, T.; David, L. Dynamic structuration of physical chitosan hydrogels. *Langmuir* **2017**, 33, 12697-12707.

(17) Lin, S. C.; Minamisawa, Y.; Furusawa, K.; Maki, Y.; Takeno, H.; Yamamoto, T.; Dobashi, T. Phase relationship and dynamics of anisotropic gelation of carboxymethylcellulose aqueous solution. *Colloid Polym. Sci.* **2010**, 288, 695-701.

(18) Furst, E. M.; Squires, T. M. *Microrheology*; Oxford University Press: New York, NY, 2017.

(19) Moschakis, T.; Lazaridou, A.; Billiaderis, C. G. Using particle tracking to probe the local dynamics of barley β-glucan solutions upon gelation. *J. Colloid Interf. Sci.* **2012**, 375, 50-59.

(20) Garting, T.; Stradner, A. Optical microrheology of protein solutions using tailored nanoparticles. *Small* **2018**, 14, 1801548.

(21) Valentine, M. T.; Perlman, Z. E.; Gardel, M. L.; Shin, J. H.; Matsudaira, P.; Mitchison, T. J.; Weitz, D. A. Colloid surface chemistry critically affects multiple particle tracking measurements of biomaterials. *Biophys. J.* **2004**, 86, 4004-4014.

(22) Meng, F.; Engbers, G. H.; Feijen, J. Polyethylene glycol-grafted polystyrene particles. *J. Biomed. Mater. Res.* **2004**, 70A, 49-58.

(23) Qian, H.; Sheetz, M. P.; Elson, E. L. Single particle tracking. Analysis of diffusion and flow in two-dimensional systems. *Biophys. J.* **1991**, 60, 910-921.

(24) Wong, I. Y.; Gardel, M. L.; Reichman, D. R.; Weeks, E. R.; Valentine, M. T.; Bausch, A. R.; Weitz, D. A. Anomalous diffusion probes microstructure dynamics of entangled F-actin networks. *Phys. Rev. Lett.* **2004**, 92, 178101.

(25) Saxton, M. J.; Jacobson, K. Single-particle tracking: applications to membrane dynamics. *Annu. Rev. Biophys. Biomol. Struct.* **1997**, 26, 373-399.

(26) Saxton, M. J. Lateral diffusion in an archipelago. Single-particle diffusion. *Biophys. J.* **1993**, 64, 1766-1780.

(27) Tsukada, T.; Kurita, R. Mechanism behind columnar pattern formation during directional quenching-induced phase separation. *Phys. Rev. Res.* **2020**, 2, 013382.

(28) Rubinstein M.; Colby, R. H. *Polymer Physics*; Oxford University Press: New York, NY, 2003.

(29) Gautieri, A.; Vesentini, S.; Redaelli, A.; Buehler, M. J. Hierarchical structure and nanomechanics of collagen microfibrils from the atomistic scale up. *Nano Lett.* **2011**, 11, 757-766.

(30) Abraham, L. C.; Zuena, E.; Perez-Ramirez, B.; Kaplan, D. L. Guide to collagen characterization for biomedical studies. *J. Biomed. Mater. Res. Part B: Appl. Biomater.* **2008**, 87B, 264-285.

(31) Tanaka, H. Hydrodynamic interface quench effects on spinodal decomposition for symmetric binary fluid mixtures. *Phys. Rev. E* **1995**, 51, 1313-1329.

(32) Tanaka, H.; Araki, T. Viscoelastic phase separation in soft matter: Numerical-simulation study on its physical mechanism. *Chem. Eng. Sci.* **2006**, 61, 2108-2141.

(33) Tanaka, H. Viscoelastic phase separation. *J. Phys.: Condens. Matter* **2000**, 12, R207-R264.

(34) Tanaka, H. Unusual phase separation in a polymer solution caused by asymmetric molecular dynamics. *Phys. Rev. Lett.* **1993**, 71, 3158-3161.

(35) Tanaka, H.; Araki, T. Phase inversion during viscoelastic phase separation: roles of bulk and shear relaxation moduli. *Phys. Rev. Lett.* **1997**, 78, 4966-4969.

Figure Captions

Figure 1. Schematic diagram of the sample chamber (side view).

Figure 2. CLSM image of MCCG of 5.0 mg/mL collagen, prepared with phosphate buffer pH 7.4.

Figure 3. Ensemble-averaged MSD for 3.0 mg/mL collagen with phosphate buffers at different pH values: pH 6.0 (○), pH 6.5 (○), pH 6.8 (○), pH 7.0 (○), pH 7.4 (○), and pH 8.0 (○), measured at 30 min after the start of dialysis. The solid line represents a straight line with a slope of 1.

Figure 4. A "phase diagram" representing the conditions for MC structure formation and gelation. The blue, green, and red circles represent MCCG, homogeneous gel, and homogeneous solution, respectively. The dashed and solid lines are guides for the eye that show the boundaries of the MC structure formation and gelation, respectively.

Figure 5. Variation of ensemble-averaged MSD at time t_d after the start of the dialysis for 5.0 mg/mL collagen and a buffer pH of 7.4. The data were obtained at t_d = 2 min (○), 4 min (○), 6 min (○), 8 min (○), 10 min (○), 12 min (○), 20 min (○), and 40 min (○). The dashed and solid lines represent straight lines with a slope of 1 and 2, respectively.

Figure 6. (a) MSD of each particle before gelation (t_d = 2 min) and the ensemble-averaged MSD of particles in the collagen solution, which are represented by gray lines and a black line, respectively. (b) MSD of each particle after gelation (t_d = 40 min). The blue, red, and green lines represent the MSD curves of solid-like, fluid-like, and intermediate behaviors, respectively. The black line represents the ensemble-averaged MSD of particles in water.

Figure 7. CLSM image of MCCG prepared with a collagen solution containing fluorescent particles (left) and a magnified image of the area marked by the dashed rectangle in the left (right). Collagen and the particles are shown in red and green, respectively. The white circles on the right indicate the particles observed in the capillaries.

Figure 8. (a) Variation of α in the short τ region (0.03 s $\leq \tau \leq$ 0.2 s) and (b) variation of the values of $\langle \Delta x^2 \rangle$ at τ = 0.09 s during MCCG formation. The filled and open circles represent the values for the majority and the diffusing particles, respectively.

Figure 9. Variation of α in the long τ region (0.5 s $\leq \tau \leq$ 2 s) during MCCG formation. The filled and open circles represent the values for the majority and the diffusing particles, respectively.

Figure 10. CLSM images of a collagen solution containing fluorescent particles during the MC structure formation. Collagen and the particles are shown in red and green, respectively. The images were obtained at t_d = 310 s (a), 320 s (b), 330 s (c), 340 s (d), 350 s (e), and 360 s (f).

Figure 11. Schematic image of substance transportation in the area where the capillary structure has newly formed.

Figure 1

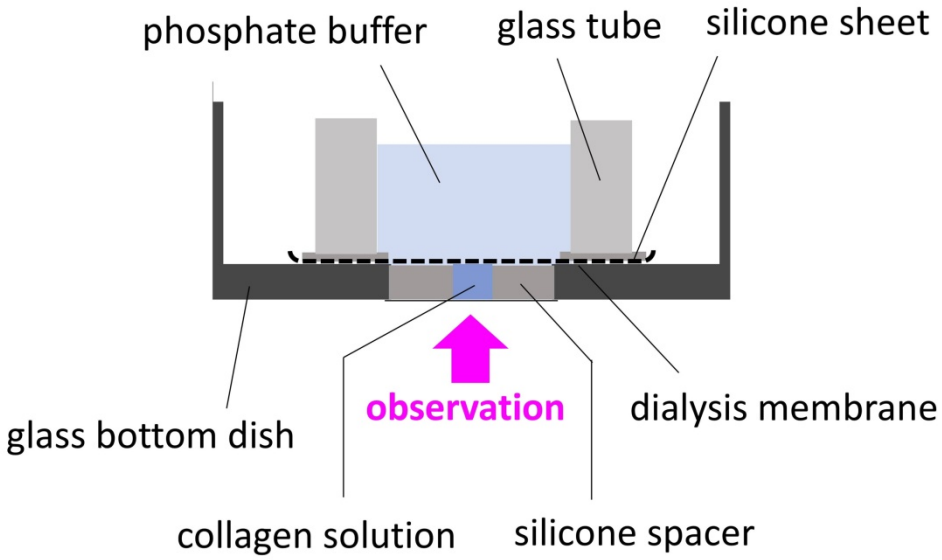
phosphate buffer
glass tube
silicone sheet
observation
glass bottom dish
dialysis membrane
collagen solution
silicone spacer

Figure 2

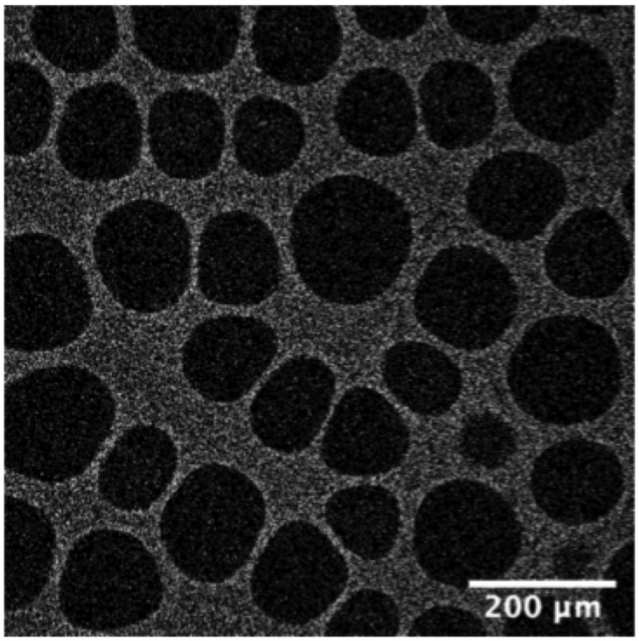

Figure 3

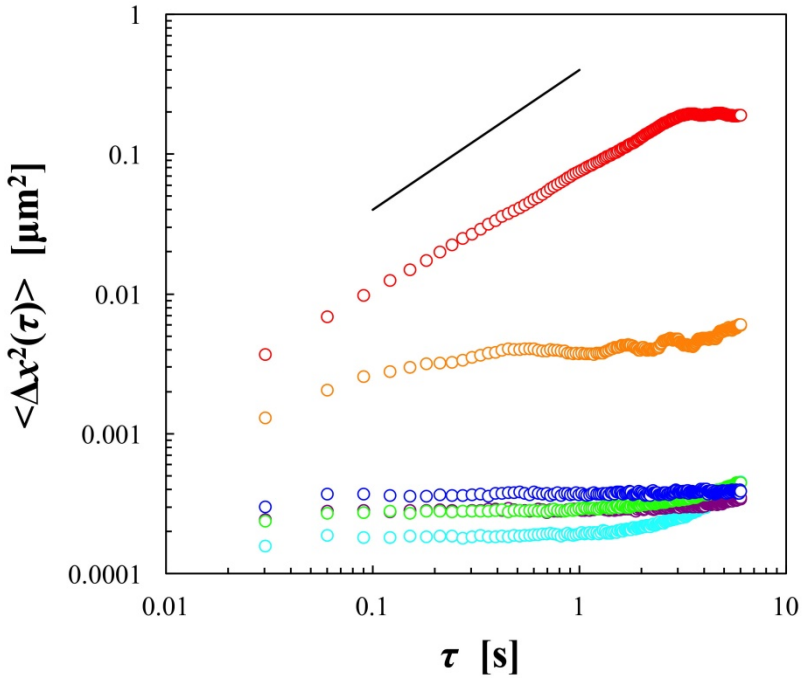
1
0.1
0.01
0.001
0.0001
0.01
0.1
1
10
$\langle \Delta x^2(\tau) \rangle$ [μm²]
τ [s]

Figure 4

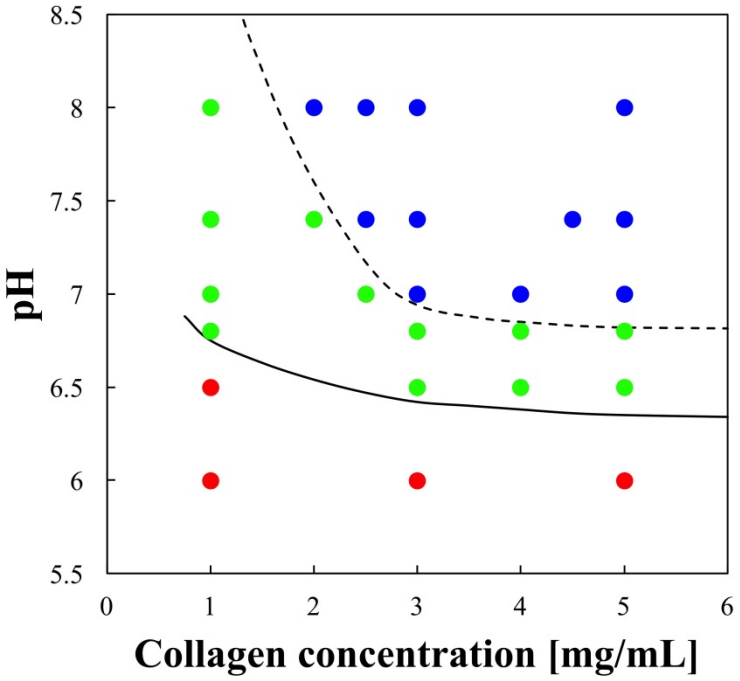

Figure 5

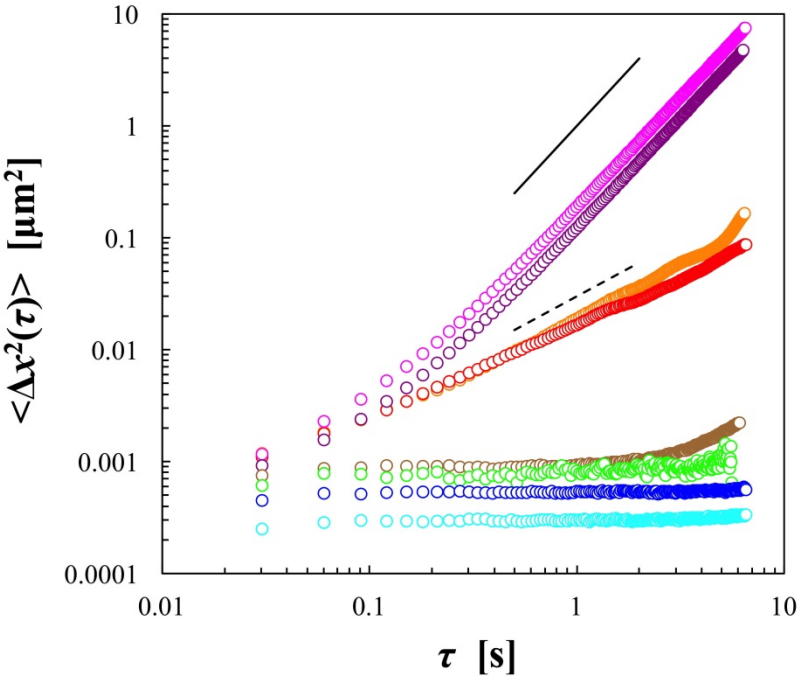

Figure 6

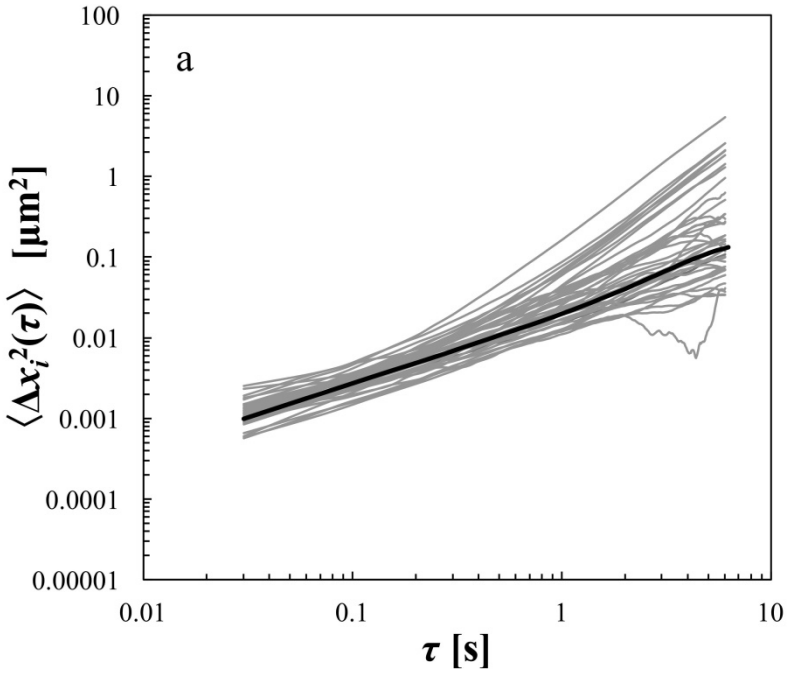
a
100
10
1
0.1
0.01
0.001
0.0001
0.00001
0.01
0.1
1
10
$\langle \Delta x_i^2(\tau) \rangle$ [μm²]
τ [s]

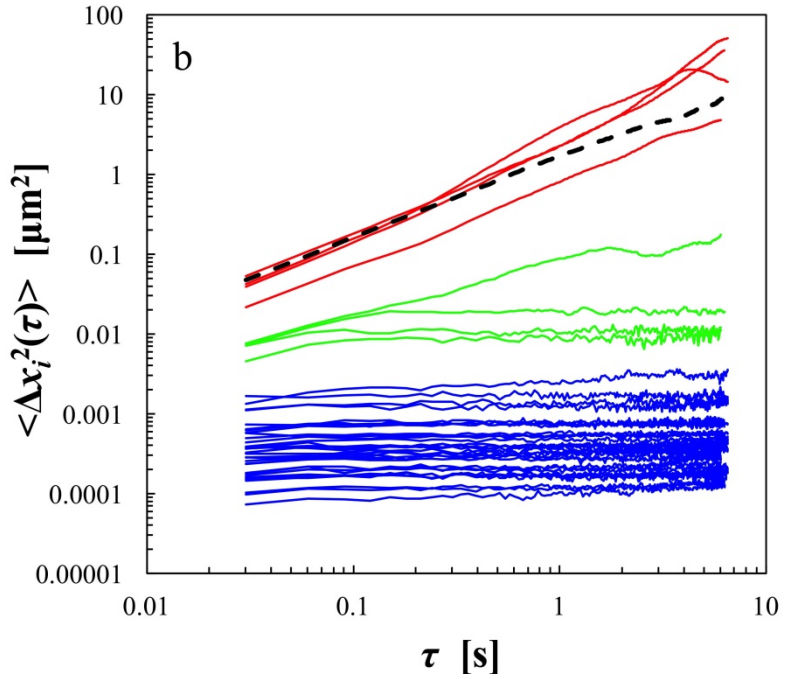
b
100
10
1
0.1
0.01
0.001
0.0001
0.00001
0.01
0.1
1
10
$<\Delta x_i^2(\tau)>$ [μm²]
τ [s]

Figure 7

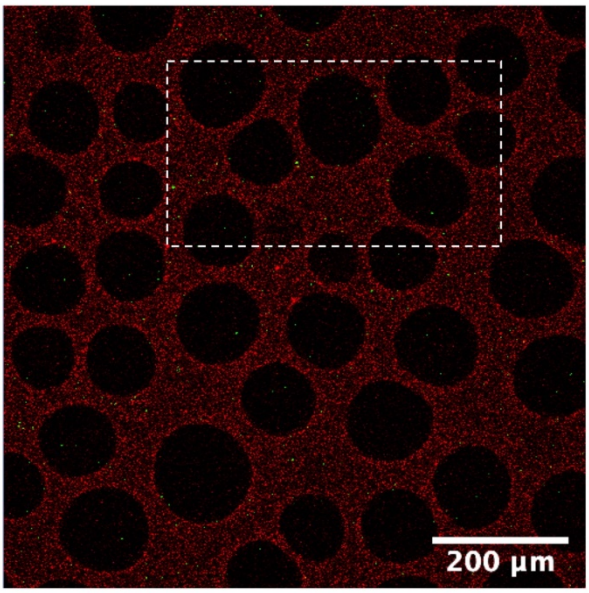

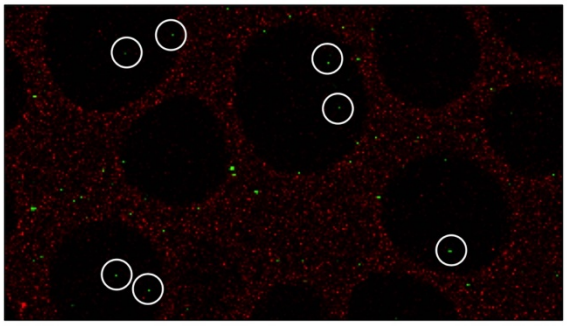

Figure 8

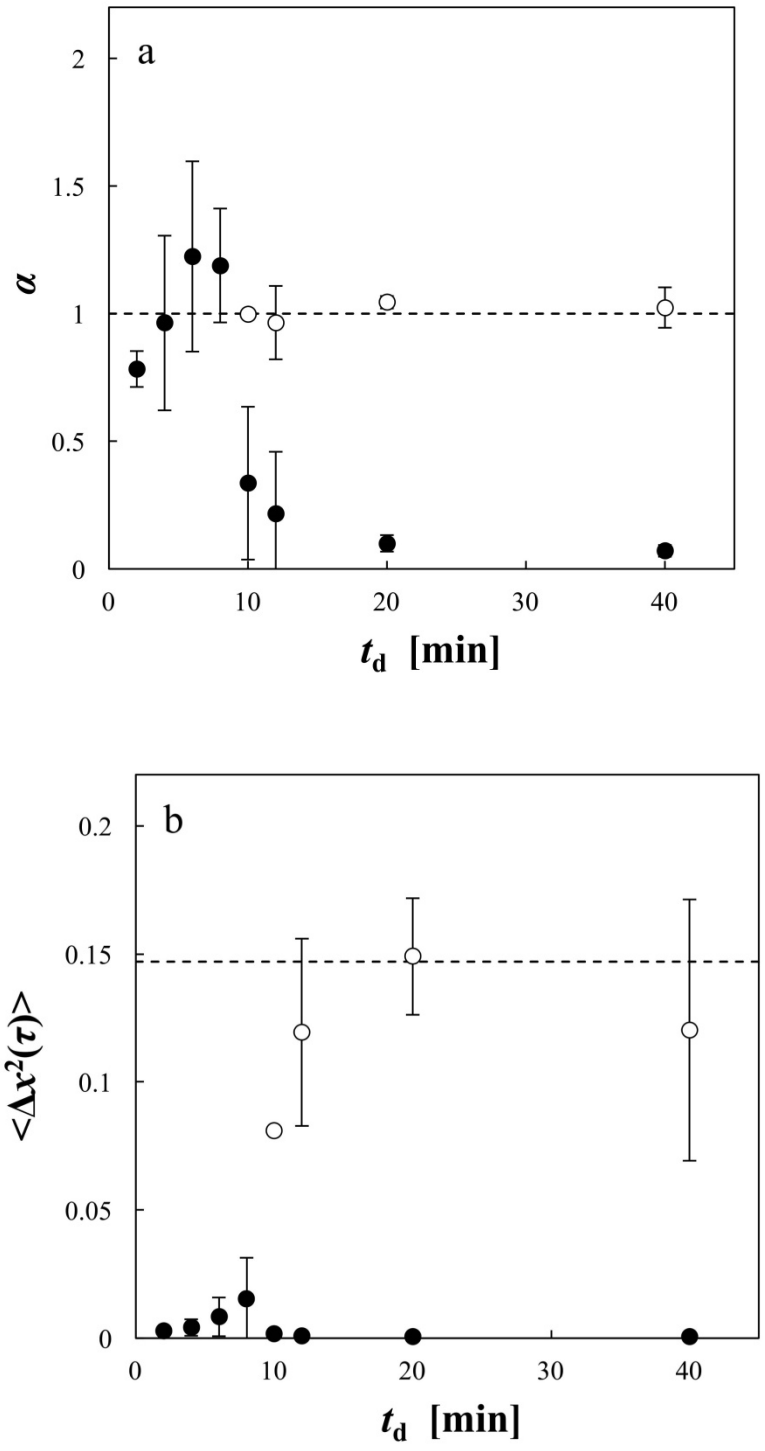
a
2
1.5
1
0.5
0
α
0
10
20
30
40
t_d [min]
b
0.2
0.15
0.1
0.05
0
$<\Delta x^2(\tau)>$
0
10
20
30
40
t_d [min]

Figure 9

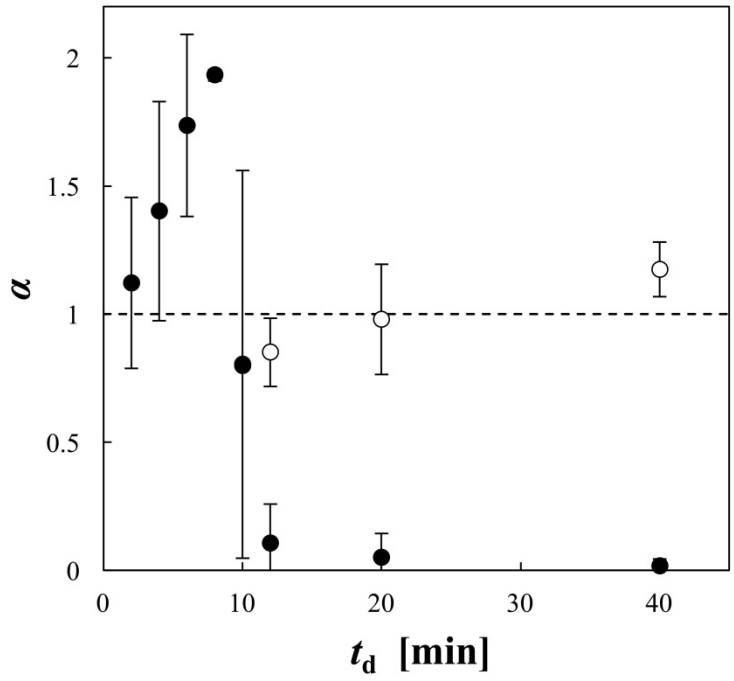

Figure 10

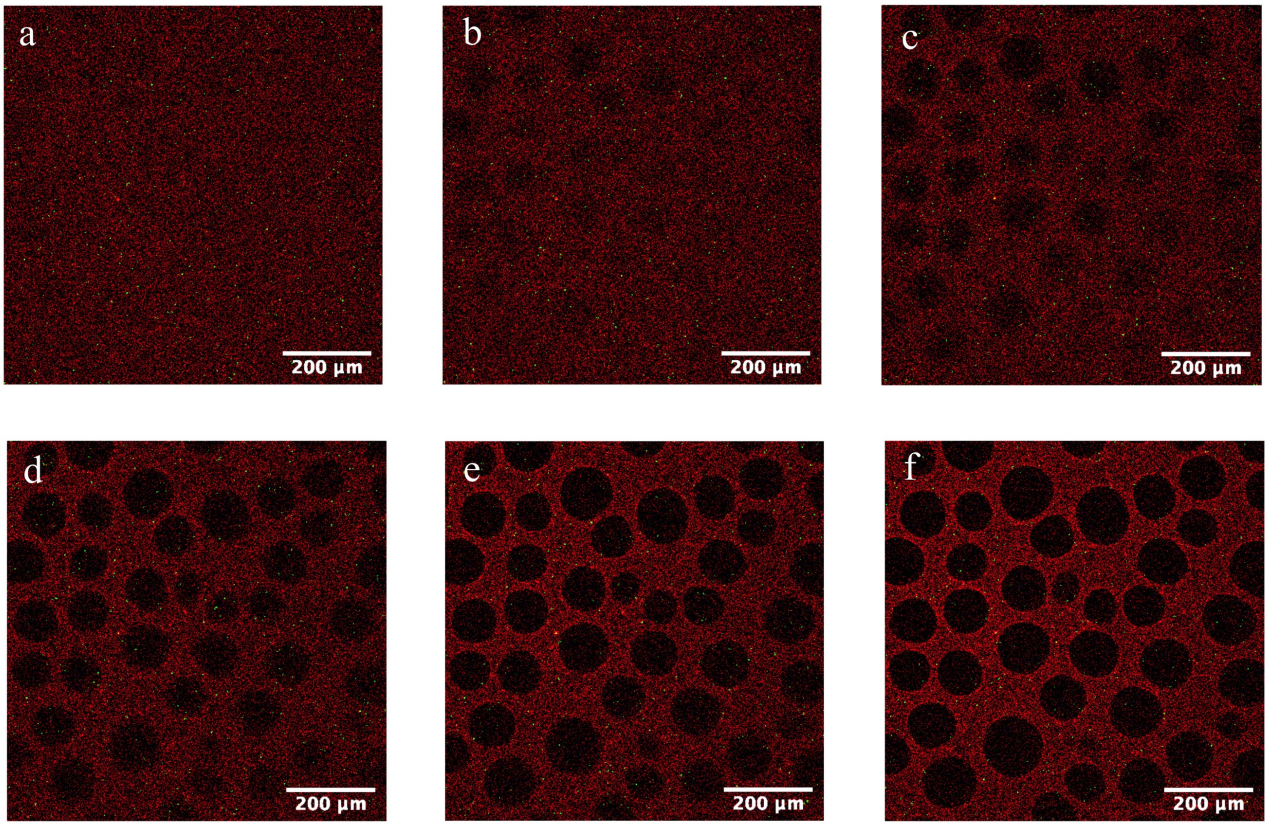

Figure 11

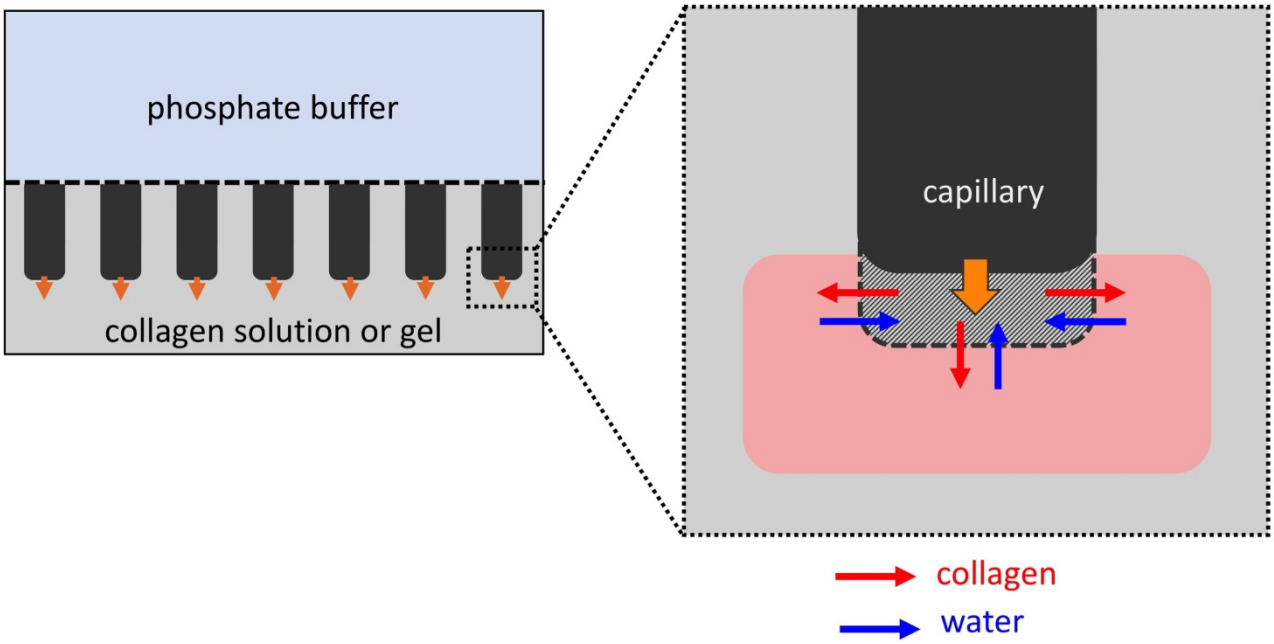
phosphate buffer
collagen solution or gel
capillary
collagen
water